

## BEAM PREPARATION FOR THE INJECTION INTO CSNS RCS\*

J.Y. Tang<sup>#</sup>, G.H. Wei, C. Zhang, J. Qiu, L. Lin, J. Wei

Institute of High Energy Physics, CAS, Beijing 100049, China

### Abstract:

The injection system of the China Spallation Neutron Source (CSNS) is designed to take one uninterrupted long drift in one of the four dispersion-free straight sections to host all the injection devices. Painting bumper magnets are used for both the horizontal and vertical phase space painting to alleviate space charge effects. To reduce beam losses at the injection and during the acceleration, the linac beam is maneuvered by a transverse collimation system and a momentum spread reduction system. The transverse collimation is carried out by triplet cells and foil strippers, which has the advantage of matched beam transfer for both the  $H^-$  and the scraped proton beams, no need for online stopping collimators and possible applications of the scraped proton beam. Multi-particle simulations using a new code to track the transfer of the mixed  $H^-$ ,  $H^0$  and proton beams have been carried. The reduction in momentum spread is carried out by a debuncher and a momentum tail collimator.

### INTRODUCTION

The main accelerator – Rapid Cycling Synchrotron (RCS) of the CSNS is a high beam power accelerator, with a design goal of 120 kW in Phase I [1-2], see Figure 1. The RCS of 1.6 GeV is fed by an injector linac of 80 MeV. The main parameters of the accelerator are shown in Table 1. Beam losses are critical in the design of the accelerator complex.  $H^-$  stripping and painting in the phase spaces are necessary measures to accumulate the required number of protons in the ring, about  $1.88 \times 10^{13}$ . The first phase of the project is expected to be completed around 2014.

Table 1: Main Parameters of CSNS RCS

	CSNS-I
Beam power (kW)	120
Repetition rate (Hz)	25
Average current ( $\mu A$ )	75
Proton energy (GeV)	1.6
Linac beam energy (MeV)	80
RCS accumulated particles	$1.9 \times 10^{13}$
RCS super-periodicity	4
RCS circumference (m)	230.8

\* Work supported by the National Natural Science Foundation of China (10775153), the CAS Knowledge Innovation Program –“China Spallation Neutron Source R&D Studies”.  
# email: tangjy@ihep.ac.cn

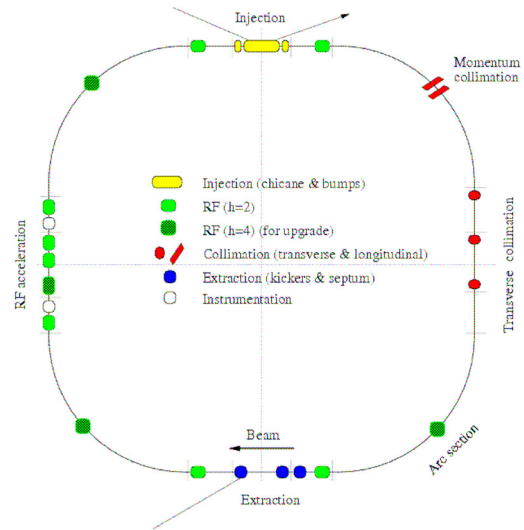


Figure 1: RCS layout and functions.

For high intensity circular proton accelerators such as the RCS, injection via  $H^-$  stripping is actually the only practical method. The design of the RCS injection system is to inject the pre-accelerated  $H^-$  beam into the RCS with high precision and high transport efficiency. At the same time, as strong space charge effects are main causes for beam losses in such high intensity accelerator, it is needed to increase the beam emittance and beam uniformity in the RCS to control the influence of the space charge effects. In order to do so, the phase space painting methods of injecting the beam of small emittance from the linac into the large ring acceptance were developed and used in the CSNS as in other similar accelerators. The injection beam with a good quality is required to further reduce the beam losses, and the cleaning of the linac beam is performed in the beam transfer line from the linac to the ring.

### INJECTION DESIGN SCHEME

Different injection schemes along with the RCS lattice schemes have been studied, and finally the design based on one long drift in a dispersion-free long straight section is favored [2-3]. A four-fold anti-symmetric lattice has been chosen for the RCS, as shown in Figure 1. The lattice functions are shown in Figure 2.

The focusing structure of the RCS long straight sections uses doublets to create a double-waist in the middle long drift of 9 m. This is helpful to reduce the strength requirements to the painting bump magnets and the foil traversal of the circulating protons. All the injection elements are accommodated within the long drift

of 9 m (see Figure 3). The design has the merits that the injection is almost independent of the ring focusing structure thus the operations such as the tune adjustment during the injection do not affect the painting process, that everything in one long drift of 9 m saves longitudinal space and avoids additional aperture requirement in the case of intercrossing with quadrupoles. The design is considered technically realizable at the CSNS, taking into account the recent development in pulsed power supplies based on IGBT for fast bump magnets.

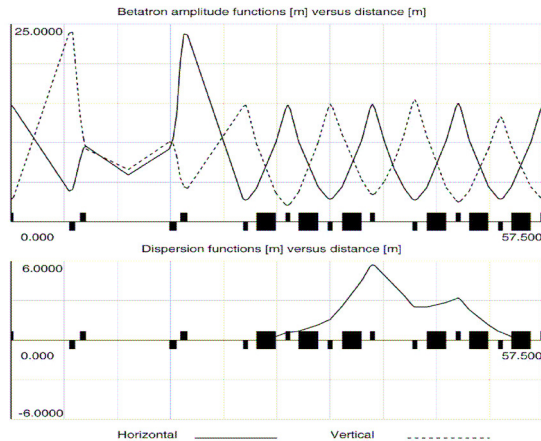


Figure 2: Lattice functions for one RCS super-period.

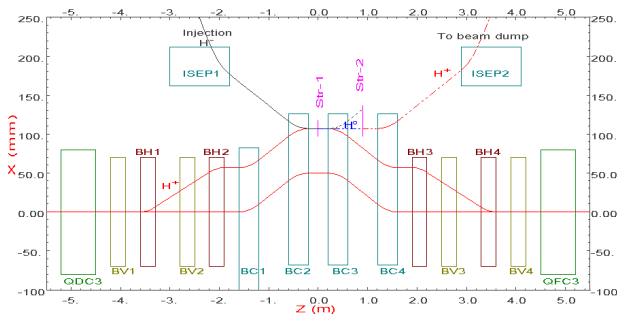


Figure 3: Layout of the RCS Injection System.

(BC1~BC4: closed-orbit DC bump magnets; BH1~BH4: horizontal painting bumpers; BV1~BV4: vertical painting bumpers; QDC3 & QFC3: ring quadrupoles; ISEP1&2: septa; Str-1 &2: stripping foils)

Two pairs of horizontal bump magnets (BH1-BH4) are for the painting in  $x$ - $x'$  plane, and two pairs of vertical bump magnets (BV1-BV4) are for painting in  $y$ - $y'$  plane. The maximum orbit bump of 40 mm in both directions allows a painting emittance of at least  $250 \pi \text{mm.mrad}$ . Whereas two pairs of horizontal bump magnets of DC type (BC1-BC4) in the middle are for additional closed-orbit shift of 50 mm (chicane magnets), and this is important for the space clearance of the injection elements. The DC type was chosen for the reason of easier vacuum design, because there are complicated vacuum connections for different beam directions in the area. To avoid excess foil traversal of the circulating

protons, the horizontal painting bump magnets are designed to have an offset bump of 17 mm in addition to the painting bump, which will collapse after the beam injection. The injection point at the main stripper is then 107 mm from the machine center. It is considered that the loss of the strict super-periodicity in the ring is not very important here. All the bumpers are powered in series for the reason of eliminating tracking errors, and they are feasible thanks to being within one drift. Another advantage of the symmetrical arrangement of the bump magnets is that the multipole components in the window-frame type magnets almost self-cancel.

Not like other modern high beam power rings such as SNS AR [4] and J-PARC RCS [5] where the non-stripped  $H^-$  and partially-stripped  $H^0$  particles at the main stripper are transported together to an injection dump, the CSNS RCS transports only the  $H^0$  particles to the injection dump and stops the non-stripped  $H^-$  particles within the injection region. The  $H^0$  particles are converted into protons by an auxiliary stripping foil (Str-2 in Fig. 3). This can avoid the complicated beam merging design for the  $H^0$  and  $H^-$  beams. To reduce the non-stripped  $H^-$  beam current to almost nothing, a transverse halo collimation method is used in the Linac Ring Beam Transport line (LRBT) to avoid the missing hit of the injection  $H^-$  particles on the foil, and this will be presented later in detail. The  $H^-$  particles absorbed at a stopper near the auxiliary stripping foil come from those passed through the foil but remained as  $H^-$ , and this represents a very small portion and is estimated to about a few Watt in beam power even in the upgrading phase. In case that the foil cracks before the lifetime, the current monitoring at the stopper will inform the control system to replace the foil.

The beam loss due to the Lorentz stripping of  $H^-$  in the bump magnets and the decay of  $H^0$  Stark states have been also studied, and it turns out that they are negligible at the injection energy of 80 MeV and not important even in the upgrading phase with an injection energy of 250 MeV.

## PHASE SPACE PAINTING

The injection with phase space painting is mandatory to reduce the tune shift due to space charge effects. According to the beam loss tolerance in different accelerators, the tune shift is controlled at about  $-0.3 \sim -0.4$  for hundreds kW accelerators and within  $-0.2$  for MW accelerators. In the RCS, the large ring physical acceptance of  $540 \pi \text{mm.mrad}$  and the collimated acceptance of  $350 \pi \text{mm.mrad}$  are used, thus the painted beam emittance is chosen to about  $250 \pi \text{mm.mrad}$ . A carefully designed painting scheme is important to control the emittance blow-up due to the space charge effects. Both correlated painting and anti-correlated painting schemes in the transverse planes have been considered for the CSNS injection system. With the correlated painting

scheme, the beam fills both the horizontal and vertical acceptance ellipses from inner to outer and the final distribution in the real space  $x$ - $y$  will be almost rectangular. With the anti-correlated painting scheme, the beam fills the vertical acceptance ellipse from outer to inner and the final distribution in  $x$ - $y$  will be elliptical. The latter is chosen as the nominal painting scheme for the CSNS, but the correlated painting scheme is kept as an alternative.

To reduce the longitudinal beam loss during the RF capture and acceleration and the transverse beam loss due to the large tune shift during the bunch shrinking, longitudinal painting schemes have been also studied by using a pre-chopped beam and off-momentum injection. It is found that the longitudinal painting does improve the beam transmission efficiency through the acceleration cycle. For example, a chopping factor of 75% (defined as macro bunch length over the chopping period) and an off-momentum of 0.35% give a good longitudinal painting result.

By using the ORBIT code [6], one can simulate the injection process including 3D space charge forces. The painting curves (orbit bump varying with time) can be optimized by using the trial and error procedure. Figure 4 shows one of the simulated results in the phase spaces at the injection end with no chopping, and Table 2 shows the statistical results. We have also introduced three parameters to describe the uniformity of a distribution in the phase spaces to help the optimization of the painting curves [7]. Fully 3D simulations including the transverse and longitudinal paintings, the injection parameters, RF voltage curve and working point are still under way. The goal is to obtain an optimized scheme that has low beam loss and fewer foil traversal of the circulating beam with reasonable hardware parameters. The foil traversal is important not only for the beam loss due to the nuclear scattering but also for the lifetime of the foil.

Case = , turn = 152

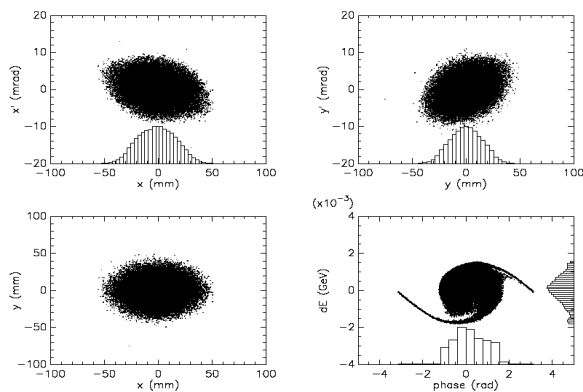


Figure 4: Beam distribution in phase spaces at the beginning of RF trapping.

(Anti-correlated,  $I_p=15\text{mA}$ ,  $V_{RF}=10\text{kV}$ , no chopping)

Table 2: Injection conditions and simulation results

Circumference (m)	230.8
Tunes ( $Q_x/Q_y$ )	5.78/5.86
$\beta_x/\beta_y$ at injection point (m)	5.61/4.35
Injection energy (MeV)	80
Injection beam peak current (mA)	15
Linac emittance $\epsilon_{x/y}$ ( $\pi\text{mm.mrad}$ , rms)	1.0
Accumulated particles	$1.88 \times 10^{13}$
Emittance at injection end (turn 117)	306/308 (99%) 273/243 (95%)
$\epsilon_x/\epsilon_y$ ( $\pi\text{mm.mrad}$ )	249/220 (90%) 63/52 (rms)

## TRANSVERSE HALO COLLIMATION IN THE LRBT

The beam halo generated in linac is considered an important source of beam losses in the ring if it is not treated properly. Some kind of transverse collimation is usually needed in the injection beam line to the ring. As  $H^-$  halo particles can be converted into protons by using stripping foils, thus it is relatively easier to remove them from the main beam. People usually use periodic FODO cells and collimators or beam dumps to remove the transverse beam halo [8-9]. At the CSNS, we have designed a collimation scheme based on periodic triplets and foil scrapers in the long straight section of the LRBT (see Figure 5) [10-11]. The reason to choose triplet cells is that they can give identical waists in both transverse planes and transport both the  $H^-$  beam and the scraped proton beam without betatron mismatch. The focusing of the  $H^-$  and proton beams looks like the exchange of the horizontal and vertical planes, thus the designed optics for the  $H^-$  beam is also perfect for the proton beam. For the comparison, a lattice based on FODO cells will give mismatched focusing for the proton beam that will result in larger beam loss or much larger aperture requirement to the quadrupole magnets. At the downstream switch magnet, the protons will be naturally separated from the  $H^-$  beam and transported either to a well-shielded beam dump or to an experimental area for proton applications with almost no beam loss in the path, the whole beam line is very clean and good for hands-on maintenance.

Two periodic triplet cells of  $60^\circ$  in phase advance in both the transverse planes and three pairs of foil scrapers in each plane at the three waists will produce a perfect hexagonal shape for the collimated beam emittance (see Figure 6). For the scraped proton beam, however, the beam distribution in both the transverse planes looks like a hollow beam plus a core beam (see Figure 7). This can be explained by the former coming from the scraping at the foils in the same plane and the latter coming from that in the orthogonal plane.

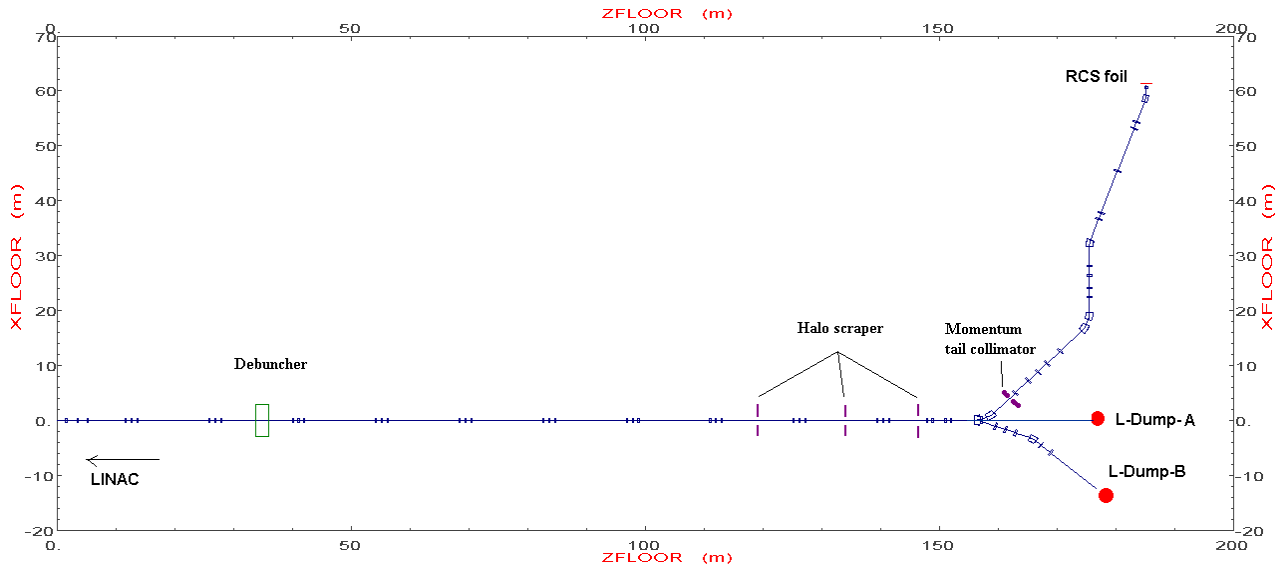


Figure 5: layout of LRBT beam transport line.

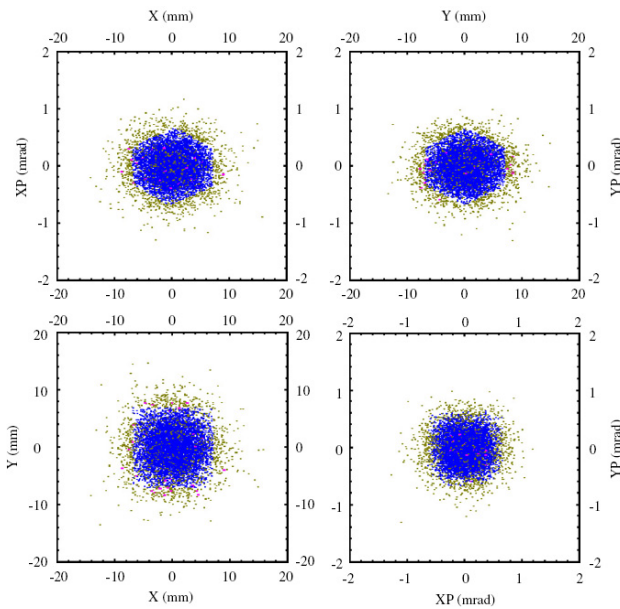


Figure 6: particle distributions in phase spaces after the three pairs of foil scrapers. (Blue:  $H^-$ ; Cyan:  $H^+$ ; Pink:  $H^0$ )

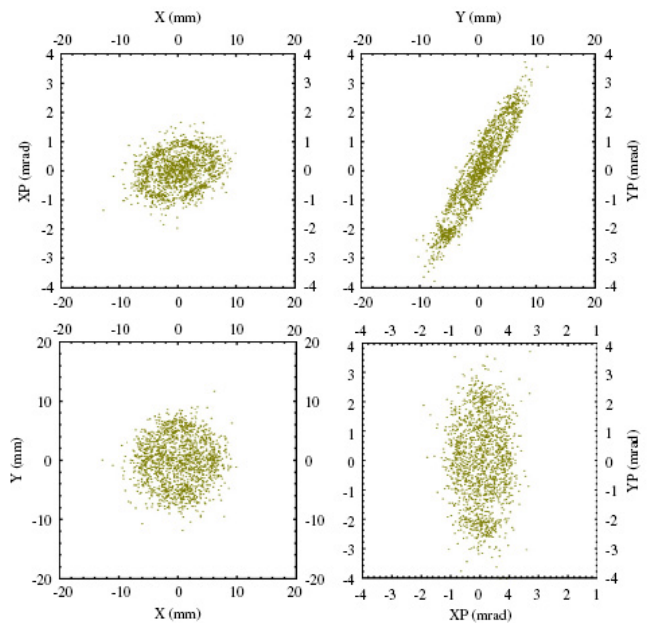


Figure 7: proton beam distribution in phase spaces after the beam separation at the switch magnet.

As the beam loss rate is at a very low level along the beam line, it allows a deep collimation to limit the beam emittance to about  $4 \pi \text{mm.mrad}$ , which is desired by the injection to avoid the missing hit of the  $H^-$  particles on the main stripping foil. This means that about 2% of the linac beam can be collimated. The transverse jitter of the linac beam has also been studied, and it turns out that this is not a critical issue for the injection, and the scraped proton beam has good intensity stability for applications.

### SIMULATIONS OF MIXED BEAM TRANSFER BY USING SCOMT CODE

As mentioned in the last section, the beam loss is of important concern in beam transport lines with some kind of transverse collimation. Due to the special features such stripping process, nuclear scattering and transfer of mixed  $H^-$  and proton beams, there is no widely used simulation code that can perform the simulation task alone. A new simulation code SCOMT (Stripping Collimation and Mixed Beam Transport), has been developed to tackle the problems [12]. The macro-particles simulation code

tracks simultaneously  $H^-$ , fully stripped proton and partially-stripped  $H^0$  beams, and takes into account the stripping processes of  $H^-$  and  $H^0$  in the foils and the multiple nuclear scattering effect in the foils. It also includes linear space charge effect. With SCOMT, it is found that the collimation method of using triplets and foil scrapers works perfectly with very little beam loss along the beam line.

An interesting fact is that main beam loss comes from the second-time hit of particles on the foils. Both scraped protons and  $H^0$  particles after passing thru a foil have a large chance to hit the downstream foils the second time. On the one hand, the second-time traverse of the protons results in larger scattering angle; on the other hand, the protons converted from the second-time stripping of  $H^0$  particles are not matched with the beam line and will be probably lost. Most of the  $H^0$  particles not hitting the foils a second time will be dumped in the straight beam dump L-Dump-A (see Figure 5). It is found that the foil thickness plays an important role in reducing the total beam loss by taking into account the second-time hits. With thinner foils, the Coulomb scattering will produce less beam loss; however, the larger portion of  $H^0$  particles due to lower stripping efficiency will also increase the beam loss. The  $H^0$  loss includes both the direct drift loss and the second-time stripping loss. With thicker foils, the Coulomb scattering at both the first-time and the possible second-time hits will result in a larger beam loss. There exists an optimum foil thickness to reduce the beam. Figure 8 shows the beam loss dependence on the foil thickness at the CSNS. The optimized foil thickness is about  $0.6 \mu\text{m}$  at 80 MeV and  $1.0 \mu\text{m}$  at 130 MeV in the upgrading phase, respectively. The beam loss power is about 0.01 W in both cases.

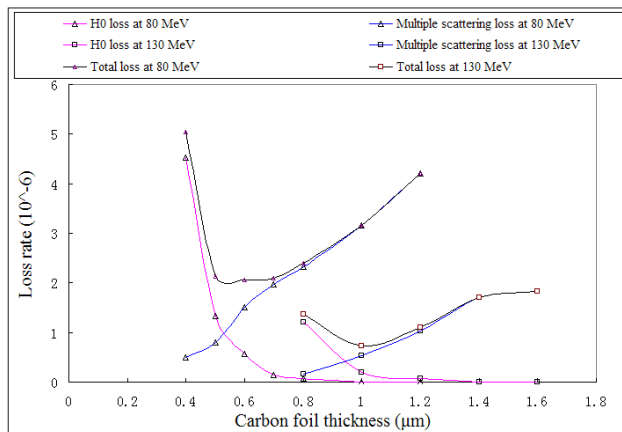


Figure 8: beam loss dependence on the foil thickness at the CSNS.

## MOMENTUM SPREAD REDUCTION

For the injection either with a continuous beam or with a chopped beam at the CSNS, a small momentum spread is helpful to reduce the longitudinal beam loss. In the former case, a small momentum spread can reduce the

beam loss during the RF capture; in the latter case, a small momentum spread can give a better longitudinal painting via the off-momentum injection. The beam at the exit of the CSNS linac has a full momentum spread of about  $\pm 0.1\%$ , but the spread will be enhanced to about  $\pm 0.3\%$  due to the longitudinal space charge effect that is dependent on the beam peak current. Therefore, a debuncher in the LRBT is designed to reduce the momentum spread to within  $\pm 0.1\%$  at the injection. The required effective RF voltage and the drift distance are about 360 kV and 30 m. The debunching effect is simulated by using PARMILA [13] (see Figure 9). The two parameters will have to be increased with higher beam energy in the upgrading phase, and the debuncher cavity will be redesigned according to higher  $\beta$ .

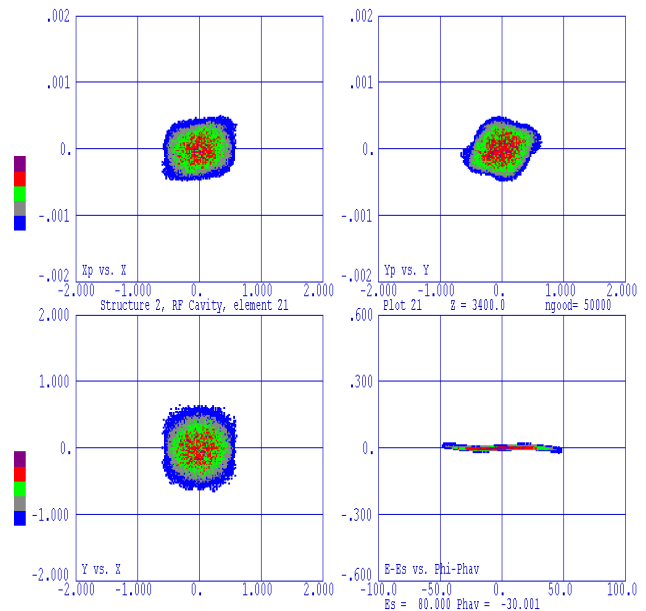


Figure 9: beam distribution in the phase spaces at the injection point after debunching.

Large momentum tail has been observed in some proton linacs and it may damage the injection devices and increase the radioactivity in the region, especially when the linac is working abnormally. Compared with normal momentum spread, this momentum tail is too large to be compensated by the debuncher, but enhanced by it due that the tail particles are in wrong phases of the debuncher. A momentum collimation in the bending section can remove all the particles with a momentum deviation of large than 0.5% (see Figure 9). The small transverse beam emittance after the collimation is helpful to increase the momentum resolution with a modest dispersion.

## CONCLUSIONS

The injection system based on one long uninterrupted drift of 9 m has been designed. The transverse painting scheme either anti-correlated or correlated has been

optimized to obtain uniform beam distribution and reduce proton traversal in the stripping foil; the longitudinal painting by using a chopped beam and off-momentum injection can help reducing the beam loss during the RF capture and acceleration. A transverse collimation system of using triplet cells and foil scrapers can limit the injection beam emittance to about  $4 \pi \text{mm.mrad}$ . The multi-particle simulations of the mixed  $\text{H}^-$ , partially stripped  $\text{H}^0$  and scraped proton beams have proven the design principle. The transverse collimation together with a debuncher and a momentum-tail collimator will result in smaller beam loss along the beam line, in the injection region and during the beam accumulation and acceleration.

### ACKNOWLEDGEMENTS

The authors would like to thank CSNS colleagues, Y.Y. Lee and D. Raparia from BNL, USA, G.H. Rees from RAL, UK for the discussion and consultations. Y.Y. Lee suggested the use of DC type chicane magnets.

### REFERENCES

- [1] CSNS accelerator team, Conceptual Design on Chinese Spallation Neutron Source -Accelerators, 2004.4, IHEP-CSNS-Report/2004-01E
- [2] J. Wei et al, China spallation neutron source accelerators: design, research and development, Proc. of EPAC 2006, Edinburgh, (2006) pp. 366-368
- [3] J.Y. Tang et al., Injection system design for the CSNS/RCS, Proc. of EPAC 2006, Edinburgh, (2006) pp.1783-1785
- [4] J. Wei et al., Injection choice for spallation neutron source ring, Proc. of PAC 2001, Chicago, (2001) pp.2560-2562
- [5] I. Sakai et al., H- painting injection system for the J-PARC 3-GeV high intensity proton synchrotron, Proc. of PAC 2003, Portland, (2003) pp.1512-1514
- [6] J. D. Galambos et al., ORBIT User Manual Version 1.10, July 1999
- [7] J. Qiu et al., Studies of Transverse Phase Space Painting for the CSNS RCS injection, HEP & NP, Vol. 31, No. 12, 2007, pp.942-946
- [8] N. Catalan-Lasheras, D. Raparia, The collimation system of the SNS transfer lines, Proc. of PAC 2001, Chicago, (2001) pp. 3263-3265
- [9] T. Ohkawa et al, Design of the beam transportation line from the LINAC to the 3-GeV RCS for J-PARC, Proc. of EPAC 2004, Lucerne, (2004) pp.1342-1344
- [10] J.Y. Tang, G.H. Wei, C. Zhang, Beam transport lines for the CSNS, Proc. of EPAC 2006, Edinburgh, (2006) pp.1780-1782
- [11] J.Y. Tang, G.H. Wei and C. Zhang, Collimation of H- beam transverse halo by triplets and foil scrapers, Nucl. Instru. and Meth. in Phys. Res. A 572 (2007) pp.601-606
- [12] G. H. Wei, J.Y. Tang and C. Zhang, Macro-particle simulation of multi-species beams in CSNS/LRBT, Nucl. Instru. and Meth. in Phys. Res. A 572 (2007) 613-617
- [13] PARMILA code: [http://laacg1.lanl.gov/laacg/services/download\\_PMI.phtml](http://laacg1.lanl.gov/laacg/services/download_PMI.phtml)